Academic Journal of Science and Technology
ISSN: 2771-3032 | Vol. 15, No. 1, 2025

Waterjet Cutting Sandstone Ability Test and Process Parameter Optimization Research

Junhao Deng[1, *]

[1]School of Energy Science and Engineering, Henan Polytechnic University, Jiaozuo, China
[*]Corresponding Author: Junhao Deng

Abstract: In China, 90% of the outburst accidents are directly related to the hard roof overburden. To enhance the top-pressure relief effect of the pre-determined directional fractures by water jet cutting, this study selected relatively hard fine-grained sandstone in the underground coal mine as the test material. Through single-factor experiments and orthogonal experiments, the influence laws of water jet process parameters (jet pressure, horizontal movement speed, cutting target distance, abrasive concentration, and cutting angle) on the rock-cutting ability were systematically analyzed. The SPH-FEM coupling method was adopted to simulate the rock-breaking process of water jet-cutting fractures. The results of single-factor experiments showed that jet pressure was positively correlated with the rock-cutting characteristic index, while lateral displacement speed was negatively correlated with it. The cutting depth showed a trend of increasing first and then decreasing with the increase of cutting target distance and abrasive concentration. The optimal target distance was 10 mm, and the optimal abrasive concentration was 12%. The cutting angle showed two depth peaks at 80° and 100°, indicating that adjusting the angle could significantly improve the cutting efficiency. The results of the four-factor five-level orthogonal experiments showed that in the case of a fixed abrasive concentration, the primary and secondary factors affecting the cutting depth were jet pressure, horizontal movement speed, cutting angle, and cutting target distance. The optimal parameter combination for water jet cutting fine-grained sandstone was jet pressure 60 MPa, horizontal movement speed 100 mm·min^{-1}, cutting target distance 20 mm, and cutting angle 85°. Based on the experimental results, a cutting-depth prediction model for fine-grained sandstone was constructed. The numerical simulation indicated that the abrasive water jet impact induced shear failure of the rock unit under the compression stress dominance, and the stress field showed a dynamic evolution characteristic of gradient attenuation from the impact center to the edge, forming an incremental damage area centered on compression failure. The prediction model and simulation results provided a theoretical basis for the optimization of water jet cutting technology, and the research results have important practical reference value for the top roof top-pressure relief engineering in coal mines.

Keywords: Waterjet; Cutting depth; Prediction model; Numerical simulation; Cutting efficiency.

1. Introduction

Coal is the "ballast stone" of China's energy system. Under the background of promoting the "dual carbon" goals, the safe and efficient mining of coal has become particularly important [1]. When the hard roof cannot collapse in time to fill the goaf and the set roof cutting support cannot effectively cut the roof, it is necessary to use pressure relief methods to promote the roof structure to reach equilibrium as soon as possible [2-6]. Water jet cutting technology has the advantages of low cost, environmental friendliness, strong applicability and high safety, and has been widely used in the cutting of coal and rock in high gas mines [7-9]. However, its cutting performance remains the main obstacle to its wide application.

At present, scholars at home and abroad have conducted in-depth research on improving the cutting capacity of the jet. Sun Lianxiang [10] and Wang Xiaochuan [11] found that the cutting capacity of the jet is closely related to factors such as jet pressure, traverse speed, cutting target distance, abrasive particle size and shape. Yu Yang [12] analyzed that the jet pressure has the greatest impact on the cutting capacity among the jet processing parameters. Hu Yang [13] found that by reasonably changing the jet impact angle, the cutting performance can be significantly improved, and there is an optimal impact angle that makes the cut depth of the target reach the maximum. Guo Jiahe et al. [14] established a cutting depth prediction model through the AWJ cutting concrete experiment; Hua Yuchang [15] established a five-order nonlinear regression prediction equation through the jet cutting 45# steel experiment, providing an accurate theoretical model for the prediction of cutting depth. Song Jinlai [16] established a depth prediction model based on jet process parameters and verified its accuracy. Liu Zhijiang [17] established a numerical model of abrasive jet impact on rock and revealed the damage and fragmentation characteristics of rock. Mi Jianyu [18] used SPH-FEM to simulate the mixing process of post-mixed abrasive water jet in the nozzle, and the final abrasive velocity can increase to 80% of the pure water velocity. Li Jinghui [19] and Meng Xiangwang [20] analyzed and verified through simulation of different processing parameters that the change trend of the single-factor jet pressure test results is consistent with that of the multi-abrasive particle simulation results. Zhao Huihe [21] compared the variation curves of the rock cutting depth with the jet rotation speed in the numerical simulation and physical experiments and found similar variation laws, proving the rationality of amplifying the jet rotation speed in the numerical simulation.

In summary, improving the cutting capacity of water jet and predicting the cutting depth of rock are still the research focuses in this field. Currently, in the coal and rock cutting engineering, due to the large differences in rock mechanical properties, the optimal process parameter combination of water jet cutting will vary with the cutting object. Therefore, this paper selects fine-grained sandstone in the extremely difficult-to-collapse hard roof in the coal mine as the cutting

target, and studies the influence laws and significant characteristics of process parameters on the cutting performance of water jet through single-factor experiments and orthogonal experiments of water jet cutting fine-grained sandstone; and establishes a prediction model of cutting depth of fine-grained sandstone based on water jet process parameters, simulates the influence of water jet process parameters on the cutting effect of fine-grained sandstone, and provides a reference for the practical application of water jet technology in the coal mine roof cutting and pressure relief engineering.

2. The Influence Law of Cutting Ability of Water Jet Cutting Fine-grained Sandstone

2.1. Test Equipment

The experiment adopted a high-pressure numerical control hydraulic cutting coal-rock test system, which mainly consists of an ultra-high-pressure water jet generator, a CNC control system, a grinding media mixed sand tank, a fully enclosed five-axis numerical control cutting platform and a data acquisition system, as shown in Figure 1. This equipment has a designed pressure of 150 MPa and a maximum flow rate of 15 L/min. The working principle of the experimental device is as follows: Water is pressurized by the ultra-high-pressure water jet generator, and the pressurized water flows through the high-pressure hose into the grinding media mixed sand tank. In this device, it is fully mixed with grinding media and accelerated by the water flow, and the mixed high-pressure grinding media jet is ejected through a Φ 1.02 cutting nozzle. The trajectory of the nozzle is controlled by the CNC system to perform cutting operations on the platform.

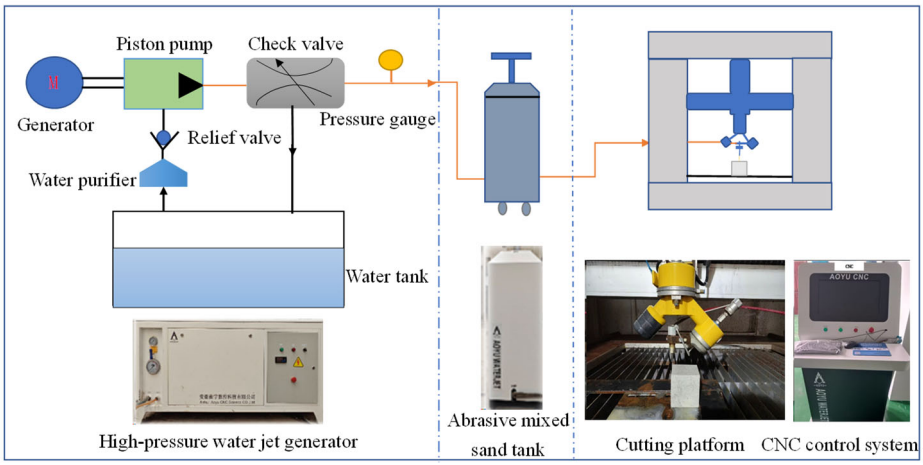

Figure 1. High-pressure CNC hydrodynamic cutting coal rock test system

2.2. Test Plan

The coal-rock mass is mainly composed of fine-grained sandstone, as shown in Figure 2. The experiment uses fine-grained sandstone from the basic top layer of the coal seam, which is difficult to collapse, as test specimens. The mechanical properties of standard rock samples were measured using the RMT150 rock mechanics testing system, with results presented in Table 1. As illustrated in Figure 3, the experiment utilized garnet abrasive with a grain size of 80 mesh (0.180 mm) and a tungsten carb.

Table 1. Test results of physical and mechanical properties of rock samples

rock sample	density (g·cm^{-3})	compressive strength (MPa)	tensile strength (MPa)	young's modulus (GPa)	poisson's ratio
Fine-grained sandstone	2.90	90	3.64	12.50	0.24

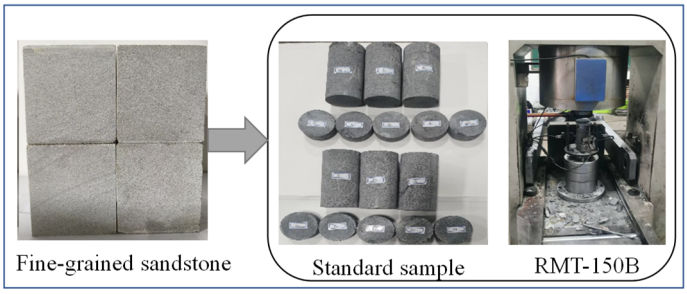

Figure 2. Photos of rock samples

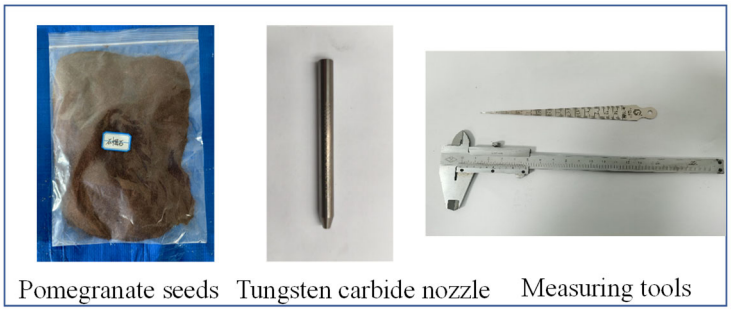

Figure 3. Materials used in the experiment

2.2.1. Key factor single-factor experiment

There are numerous process parameters that affect waterjet cutting performance. Based on previous research findings and the actual conditions of coal mine underground cutting projects, this experiment primarily focuses on the impact of cutting depth and kerf width in relation to factors such as jet pressure, cutting distance, abrasive concentration, traverse speed, and cutting angle. The values for relevant parameters during the waterjet cutting tests are listed in Table 2.

Table 2. Test results of physical and mechanical properties of rock samples

Process parameters	Range of values
Nozzle diameter（*D*/mm）	1.02
Abrasive particle size（*d*/mesh）	80
Jet pressure（*P*/MPa）	10、20、30、40、50、60
Horizontal movement speed（*V*/mm·min^{-1}）	100、200、300、400、500、600
Abrasive concentration/(*C*/%)	4、8、12、16、20
Cutting target distance（*L*/mm）	5、10、15、20、25、30
Cutting angle（ δ/°）	75°、80°、85°、90°、95°、100°、105°

2.2.2. Orthogonal experiment of key factors

This paper uses an L25(54) orthogonal experiment to investigate various factors affecting waterjet cutting depth, including jet pressure, traverse speed, cutting target distance, and cutting angle. These factors are divided into five levels for fine-grained sandstone cutting experiments. Detailed orthogonal experiment tables can be found in Table 3.

Table 3. Orthogonal test parameters and their values

Experimental parameters	Level 1	Level 2	Level 3	Level 4	Level 5
Jet pressure (*P*/MPa)	20	30	40	50	60
Horizontal movement speed (V/mm·min^{-1})	100	200	300	400	500
Cutting target distance (*L*/mm)	5	10	15	20	25
Cutting angle (δ/°)	70	80	90	100	110

3. Results Analysis

3.1. Analysis Of Single-factor Experimental Results

3.1.1. The effect of jet pressure on seam characteristics

Under fixed operating parameters (horizontal movement speed of 200 mm·min-1, cutting angle of 90°, cutting target distance of 10 mm, abrasive concentration of 12%), the effect of jet pressure on the cutting morphology was studied by adjusting the jet pressure. As shown in Figure 4, the kinetic energy of the abrasive particles significantly increases, enhancing their ability to erode and break down the rock. However, when the jet pressure exceeds 30 MPa, the rate of increase in cutting depth begins to slow down. This is mainly due to two reasons: first, excessively high pressure intensifies collisions between abrasive particles and between particles and the nozzle inner wall, causing some abrasive particles to break, thereby weakening the cutting capability of the abrasive jet; second, as the jet propagates through the air and enters the cut seam, it encounters resistance and buffering from the solid-liquid mixture, gradually slowing down the rate of increase in cutting depth. At the same time, when the jet pressure exceeds 30 MPa, the rate of increase in cut seam width starts to accelerate. This is because with increasing jet pressure, the flow rate per unit time increases, leading to more intense collisions between abrasive particles, making the reflected abrasive jet more chaotic and resulting in an increase in cut seam width.

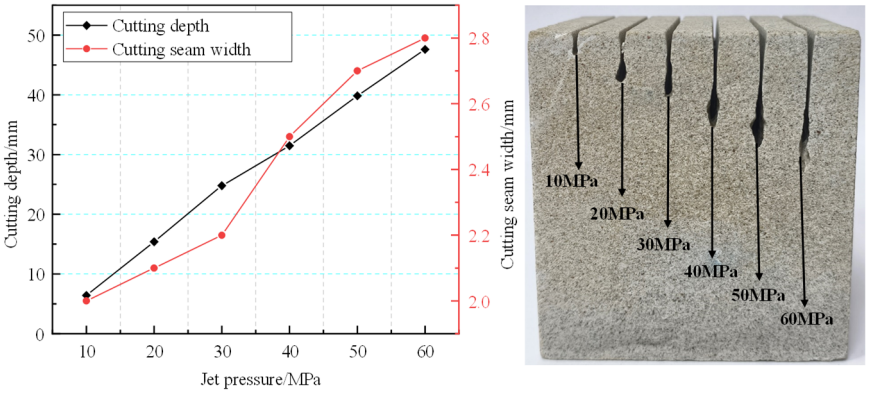

Figure 4. Relationship between jet pressure and slit characteristics

3.1.2. The effect of horizontal movement speed on seam characteristics

Under fixed operating parameters (jet pressure of 50 MPa, cutting angle of 90°, cutting target distance of 10 mm, abrasive concentration of 12%), the effect of nozzle traverse speed on the cutting morphology was studied by adjusting the traverse speed. As shown in Figure 5, both cutting depth and kerf width are negatively correlated with traverse speed, and their reduction rate slows down as traverse speed increases. An increase in traverse speed shortens the cutting time per unit length, reducing the number of abrasive impacts on the target per unit time, thereby weakening the erosion capability and.

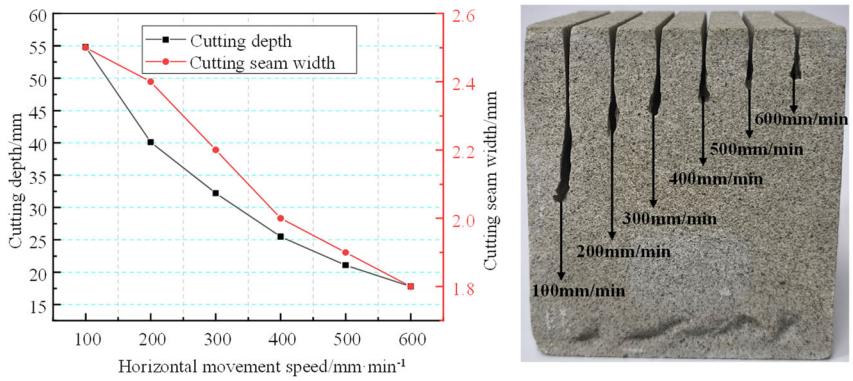

Figure 5. Relationship between horizontal movement speed and slit characteristics

3.1.3. The effect of abrasive concentration on cutting seam characteristics

Under fixed process parameters (horizontal movement speed of 200 mm·min^{-1}, jet pressure of 50 MPa, cutting angle of 90°, and cutting target distance of 10 mm), the effect of abrasive concentration on the cutting morphology was studied by adjusting the abrasive concentration. As shown in Figure 6, the impact of abrasive concentration on cutting performance parameters exhibits significant nonlinear characteristics. When the abrasive concentration is below 12%, both cut seam depth and width increase with increasing abrasive concentration; however, when the abrasive concentration exceeds 12%, the cut seam depth and width decrease instead, indicating that 12% is the optimal abrasive concentration for cutting sandstone. This is because when the abrasive concentration reaches saturation, on one hand, the frequency of collisions and friction between abrasive particles increases, reducing the number of effective cutting particles per unit volume of the jet, thereby weakening the impact grinding effect; on the other hand, higher abrasive concentrations result in more solid-liquid mixtures at the bottom of the cut seam, hindering the energy transfer of subsequent jet particles, thus reducing the cutting depth.

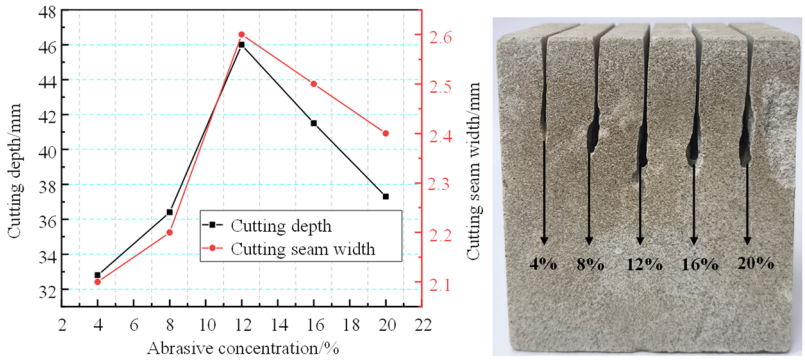

Figure 6. Relationship between abrasive concentration and slit characteristics

3.1.4. The effect of cutting target distance on seam characteristics

Under fixed process parameters (horizontal movement speed 200 mm·min^{-1}, jet pressure 50 MPa, cutting angle 90°, abrasive concentration 12%), the effect of varying the cutting target distance on the cutting morphology was studied. As shown in Figure 7, within the range of 0 to 10 mm for the cutting target distance, the jet is affected by rebound particles, weakening its impact effect, resulting in a positive correlation between cutting depth and cutting target distance. When the cutting target distance continues to increase, the mutual interference of the jets and the disturbance of the rebounding jet gradually decrease, eventually becoming negligible. The axial velocity and dynamic pressure of the jet gradually diminish, reducing kinetic energy, leading to a negative correlation between cutting depth and cutting target distance beyond 10 mm. Additionally, the jet diameter diverges with increasing cutting target distance, causing the cut seam width to have a positive correlation with the cutting target distance.

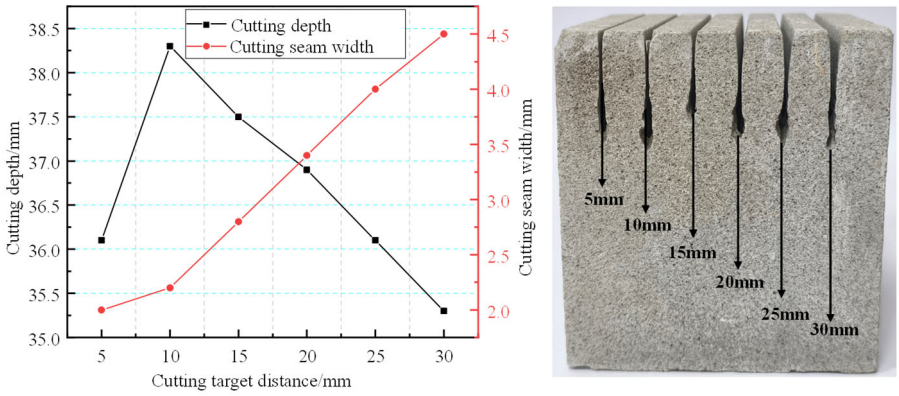

Figure 7. Relationship between cutting target distance and slit characteristics

3.1.5. The effect of cutting angle on seam characteristics

Under fixed process parameters (horizontal movement speed 200 mm·min^{-1}, jet pressure 50 MPa, cutting target distance 10 mm, abrasive concentration 12%), the effect of cutting angle on the cutting morphology was studied by adjusting the cutting angle. As shown in Figure 8, when the cutting angle is 90°, the cutting effect is the worst; at cutting angles of 80° and 100°, there are two peaks in cutting depth and cut seam width. Changing the waterjet cutting angle effectively mitigates the impact of abrasive particle rebound on jet cohesiveness to some extent, thereby improving the rock-cutting efficiency of the waterjet.

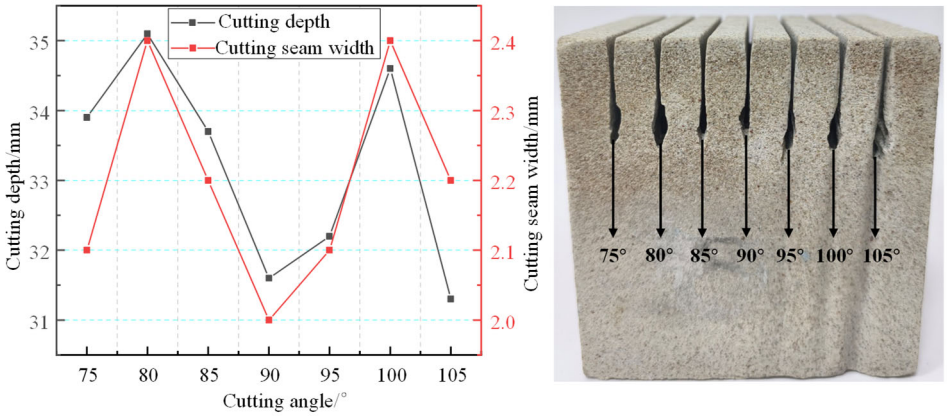

Figure 8. Relationship between cutting angle and slit characteristics

3.2. Orthogonal Experiment Results and Analysis

The target material used in the orthogonal experiment is the same fine-grained sandstone as that used for the single-factor cutting targets. The cutting depth H is used as the evaluation criterion. The results of the orthogonal experiment are shown in Table 4.

Table 4. Orthogonal experimental results

Number	*L*/mm	*P*/MPa	*V*/mm·min^{-1}	*δ*/°	*H*/mm
1	5	20	100	80	19.64
2	5	30	300	95	18.84
3	5	40	500	85	18.08
4	5	50	200	100	38.28
5	5	60	400	90	27.92
6	10	20	500	95	7.60
7	10	30	200	85	24.72
8	10	40	400	100	18.20
9	10	50	100	90	47.82
10	10	60	300	80	33.80
11	15	20	400	85	8.56
12	15	30	100	100	34.85
13	15	40	300	90	23.84
14	15	50	500	80	21.00
15	15	60	200	95	41.92
16	20	20	300	100	9.72
17	20	30	500	90	12.80
18	20	40	200	80	30.88
19	20	50	400	95	22.64
20	20	60	100	85	67.48
21	25	20	200	90	16.48
22	25	30	400	80	12.64
23	25	40	100	95	44.08
24	25	50	300	85	31.44
25	25	60	500	100	23.16

Based on the experimental results, a sensitivity analysis of the cutting depth was conducted. Using the cutting depth experimental data from Table 4, the mean and range values for each factor at different levels were calculated, as shown in Table 5.

Table 5. Analysis of cutting depth range

Item	Number	*L*	*P*	*V*	*δ*
K value	1	122.76	62	213.87	117.96
	2	132.14	103.85	152.28	150.28
	3	130.17	135.08	117.64	128.86
	4	143.52	161.18	89.96	135.08
	5	127.80	194.28	82.64	124.21
ki value	1	24.55	12.40	42.77	23.59
	2	26.43	20.77	30.46	30.01
	3	26.03	27.01	23.53	25.77
	4	28.70	32.24	17.99	27.02
	5	25.56	38.86	16.53	24.84
R		4.15	26.46	26.24	6.42
Primary importance			P>V>*δ*>L		

As shown in Figure 9, the factors influencing cutting depth, in descending order of impact, are jet pressure, horizontal movement speed, cutting angle, and cutting target distance. The optimal cutting parameters for waterjet cutting of fine-grained sandstone were determined to be a jet pressure of 60 MPa, a horizontal movement speed of 100 mm/min, a jet-target distance of 20 mm, and a cutting angle of 85 degrees.

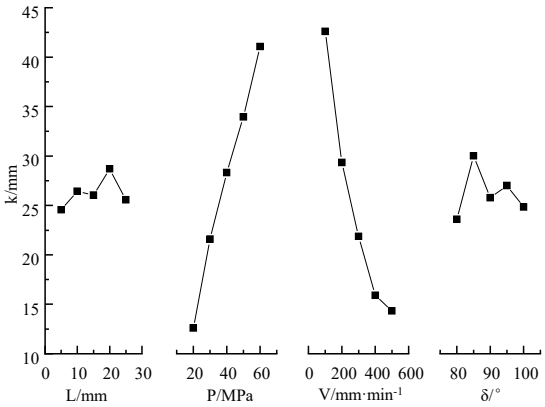

Figure 9. Trend chart of slot depth range

3.3. Cutting Depth Prediction Model

To quantitatively analyze the changes in cutting depth under the combined influence of four parameters: jet pressure, horizontal movement speed, cutting target distance, and cutting angle, we established a cutting depth prediction model based on multiple linear regression. The process of multiple linear regression is as follows:

$$H = AP^{a_1}V^{a_2}L^{a_3}\delta^{a_4}. \quad (1)$$

In the formula: A is a constant coefficient; Taking logarithms on both sides of formula (1) yields:

$$\ln H = \ln A + a_1 \ln P + a_2 \ln V + a_3 \ln L + a_4 \ln \delta. \quad (2)$$

Order: $\ln H = \mathrm{y}$, $\ln A = a_0$, $\ln P = a_1$, $\ln V = a_2$, $\ln L = a_3$, $\ln \delta = a_4$ .Transform equation (2) into the general expression of multiple linear regression:

$$y = a_0 + a_1x_1 + a_2x_2 + a_3x_3 + a_4x_4. \quad (3)$$

$$\text{Order}: \quad y = \begin{bmatrix} y_1 \\ y_2 \\ \vdots \\ y_{25} \end{bmatrix}; \quad a = \begin{bmatrix} a_1 \\ a_2 \\ \vdots \\ a_n \end{bmatrix}; \quad c = \begin{bmatrix} c_1 \\ c_2 \\ \vdots \\ c_n \end{bmatrix}; \quad x = \begin{bmatrix} 1 & x_{11} & x_{12} & x_{13} & x_{14} \\ 1 & x_{21} & x_{22} & x_{23} & x_{24} \\ \vdots & \vdots & \vdots & \vdots & \vdots \\ 1 & x_{251} & x_{252} & x_{253} & x_{254} \end{bmatrix}_{25\times5}$$

Let c be a random variable (for i = 1, 2, 3, ..., 25). Therefore, we have:

$$y = ax + c. \quad (4)$$

Using the least squares method, the above matrix was solved based on orthogonal test data using Matlab software. The results of the model solution are shown in Table 6.

Table 6. Results of model solution

Regression parameters	Value	Confidence interval
A	25.894 0	[-29.718 8, 81.506 9]
a1	0.964 1	[0.851 6, 1.076 5]
a2	-0.580 9	[-0.637 2, -0.524 6]
a3	0.027 2	[-0.036 8, 0.091 1]
a4	-0.096 5	[-0.545 8, 0.352 7]
Statistic	R^2=0.977 8, F=220.548 9, P=0, S^2=5.253 3	

Based on the R-squared and p-value from the calculated statistics, the regression equation fits the experimental data well, indicating a certain level of accuracy in the regression analysis results. Combining (2) and (3), the regression equation is as follows:

$$H = 25.894P^{0.9641}V^{-0.5809}L^{0.0272}\delta^{-0.0965} \quad (5)$$

The regression equation indicates that cutting depth increases with higher jet pressure but decreases with increased traverse speed, which aligns with the results of orthogonal test analysis. The primary factors affecting the cutting depth of fine-grained sandstone, in descending order of influence, remain jet pressure, traverse speed, cutting angle, and cutting distance. The predictive model accurately reflects real-world conditions and provides valuable guidance for predicting rock cutting depth on-site.

4. Numerical Analysis of Waterjet Cutting Rock Seams

4.1. Calibration Of Numerical Model Parameters

As shown in Figure 10, the model establishment mainly includes two parts: the first part is jet modeling. Initially, a geometric model of a jet with a diameter of 1 mm and a length of 50 mm is constructed and meshed. Using a Python script, grid nodes are randomly selected based on the proportion of abrasive material, setting the abrasive mass concentration to 12%. The selected nodes are assigned abrasive properties, while the remaining nodes are assigned water properties. Additionally, the initial velocity v is set for the jet, along with the state equation parameters for water and mechanical parameters for the abrasive. The second part is rock modeling. A cube-shaped rock with dimensions of 100 mm × 100 mm × 100 mm is defined and given material parameters (using the Drucker-Prager model). Subsequently, the model assembly and meshing are performed, and the mesh in the impact cutting region is refined to a cubic grid with an edge length of 0.04 mm. Finally, the bottom of the rock model is set as a fixed constraint.

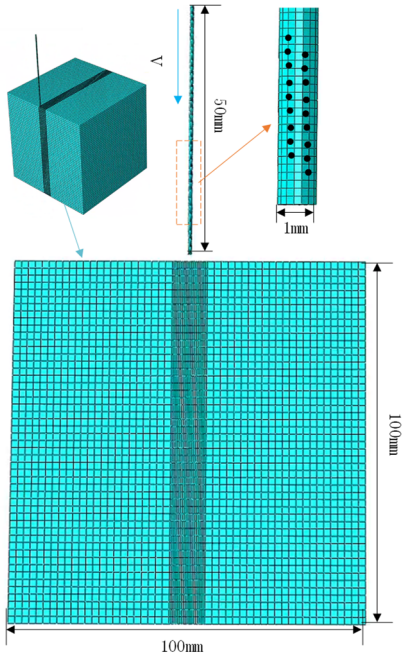

Figure 10. Schematic diagram of the numerical model

4.2. Numerical Model Validation

To ensure that the established waterjet cutting rock numerical model accurately simulates the cutting effect observed in physical experiments, the macroscopic parameters of rock cutting obtained from the experiment were used to validate the numerical model. In the numerical

simulation, the process of rock element fragmentation and deletion occurs on a microsecond scale, whereas in actual experiments, rock fragmentation happens on a second scale. As shown in Figure 11, through multiple comparisons between numerical simulations and experimental results, it was found that when the lateral speed in the numerical simulation is set to 20,000 times that of the experiment, the simulation results align closely with the experimental observations of how the depth of rock cutting varies with lateral speed.

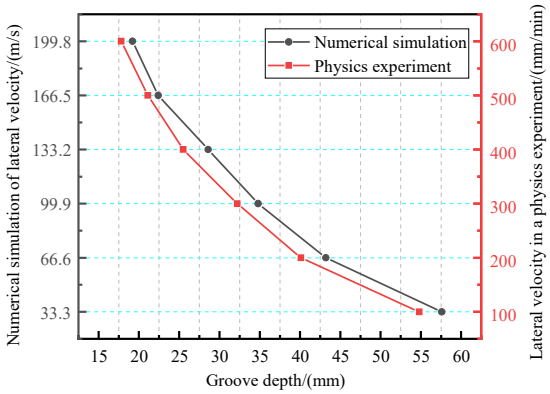

Figure 11. Relationship diagram between cutting depth and horizontal movement speed

To further verify that amplifying the lateral traverse speed can accurately simulate the process of abrasive waterjet cutting rock joints in numerical simulations, a comparison was made between the rock cutting depth obtained from physical experiments and numerical simulations with amplified traverse speed under identical working parameters. As shown in Figure 12, taking fine-grained sandstone as an example, in the physical experiment, the jet pressure was 50 MPa, the standoff distance was 10 mm, the abrasive concentration was 12%, the traverse speed was 500 mm·min^{-1}, and the cutting angle was 90°. Under these conditions, the measured depth of rock cutting by the abrasive waterjet in the physical experiment was 21.1 mm, while the numerical simulation yielded a rock cutting depth of 22.4 mm, with an error of 6.2%. This indicates that the numerical model established in this study can accurately simulate the process of abrasive waterjet rotary cutting of rock joints. By analyzing the effect of abrasive waterjet working parameters on the rock cutting depth through amplified traverse speed, the results conform to the error requirements of the numerical simulation experiment.

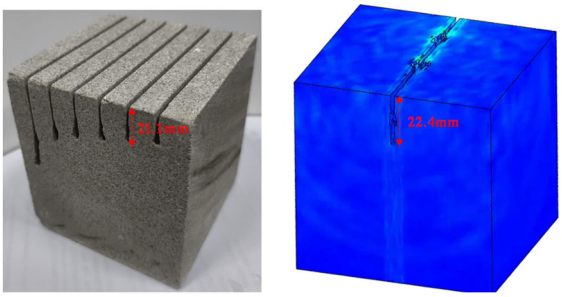

Figure 12. Comparison chart of physical experiment and numerical simulation

4.3. Waterjet Cutting Simulation Process

The jet pressure was set at 20 MPa, and the simulation results of jet cutting at four different moments are shown in Figure 13. During the process of jet cutting fine-grained sandstone, the kinetic energy of the jet is converted into impact force acting on the rock surface, initially creating compressive stress, especially in the local area where water flow impacts; at this point, the rock surface deforms, and the stress in the local area exceeds the rock's elastic limit, initiating micro-cracking. As the impact force increases, the internal stress field of the rock changes, with shear stress acting on areas beneath the rock surface, causing the rock to break or for cracks to expand, particularly in regions with higher pressure. The high-speed flow of the water jet not only affects the rock surface but also generates stress waves within the rock, these impact waves propagate through the rock, gradually diminishing from the main impact area to the surroundings, causing stress concentration within the rock, further promoting crack propagation. When the compressive and shear stresses caused by the water jet's impact exceed the rock's compressive strength or shear strength, the units on the rock's surface and interior fail. These failed units are removed from the rock, forming a cutting path. Under continuous jet impact, local micro-cracks gradually expand, eventually forming larger fractures. Micro-cracks within the rock extend along the direction of maximum stress and coalesce into a macroscopic crack, leading to the cutting of the rock.

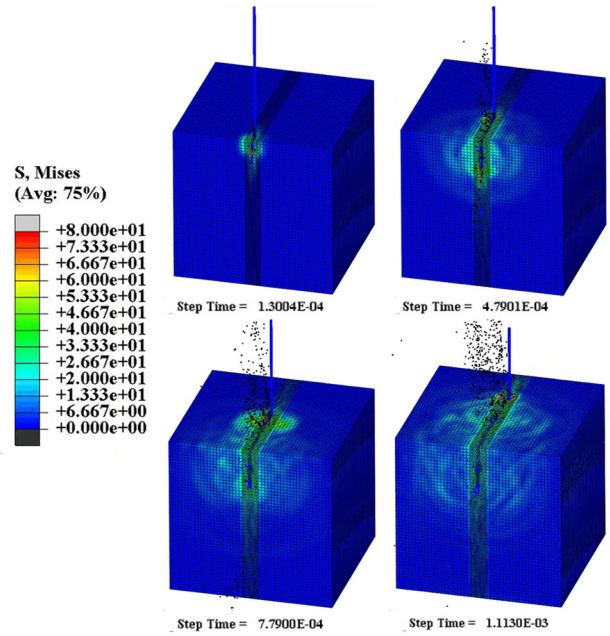

Figure 13. Simulation process of jet cutting

4.4. Comparison and Analysis of Simulation Results and Experimental Results Under Different Jet Pressures

Under conditions of a horizontal movement speed of 200 mm·min-1, cutting target distance of 10 mm, impact angle of 90°, and abrasive concentration of 12%, the variation in rock cutting depth with increasing waterjet pressure was simulated by setting the initial speed of the abrasive. Figures 14 and 15 show the simulation results for jet pressures of 20 MPa and 30 MPa, respectively.

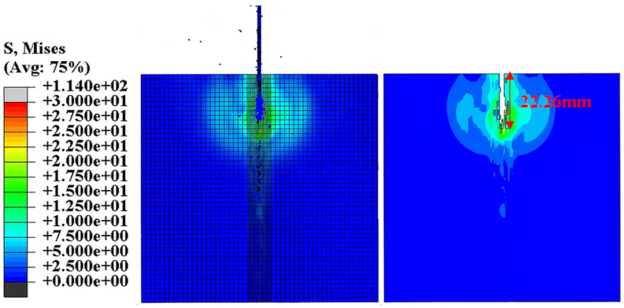

Figure 14. Simulation results of jet pressure 20MPa

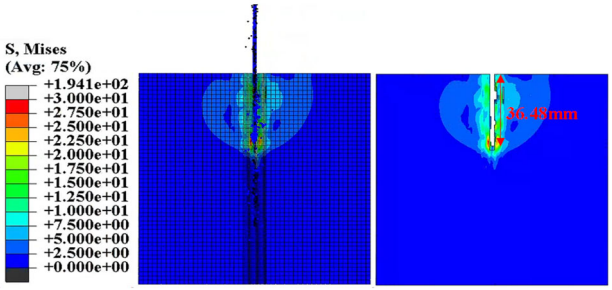

Figure 15. Simulation results of jet pressure 30MPa

The comparison of jet simulation cutting depths at different jet pressures and single-factor test cutting depths is shown in Table 7.

Table 7. Results of model solution

P/MPa	10	20	30	40	50	60
Test cutting depth (mm)	6.40	15.40	24.78	31.48	39.84	47.60
Simulated cutting depth (mm)	12.12	22.26	36.48	42.42	46.16.	54.82

As shown in Figure 16, the cutting depth of the jet simulation increases nonlinearly with increasing jet pressure. Within the range of 10 MPa to 30 MPa, the 'water hammer pressure' and the high-frequency impact of abrasive particles are the main reasons for the rapid increase in rock cutting depth. Within the range of 30 MPa to 50 MPa, although the rock cutting depth continues to increase, the stagnation pressure of the abrasive water jet within the rock fissures has limited rock-breaking capability, and the presence of solid-liquid mixtures within the fissures causes a decline in the impact velocity of the abrasive water jet, resulting in a relatively slower increase in rock cutting depth. When the jet working pressure exceeds 50 MPa, the solid-liquid mixture within the rock fissures similarly weakens the impact velocity of subsequent abrasive water jets; however, under higher impact dynamic pressure, the stagnation pressure within the rock fissures significantly increases, which is beneficial for secondary fracturing of the rock, possibly being the main reason for the rapid increase in rock cutting depth once again.

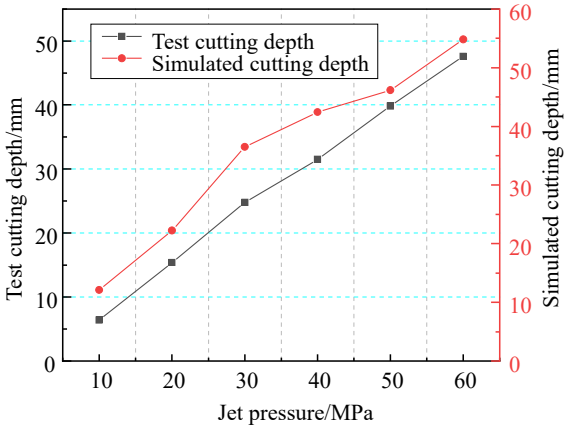

Figure 16. Comparison of test and simulation results for jet pressure

4.5. Comparison And Analysis of Simulation Results and Experimental Results Under Different Horizontal Movement Speeds

Under conditions of jet pressure at 50 MPa, abrasive concentration at 12%, cutting target distance at 10 mm, and impact angle at 90°, the variation pattern of rock cut seam depth with increasing waterjet traverse speed was analyzed by amplifying the waterjet traverse speed. As shown in Figures 17 and 18, the simulation results for horizontal movement speeds of 300 mm·min-1 and 400 mm·min-1 are presented respectively.

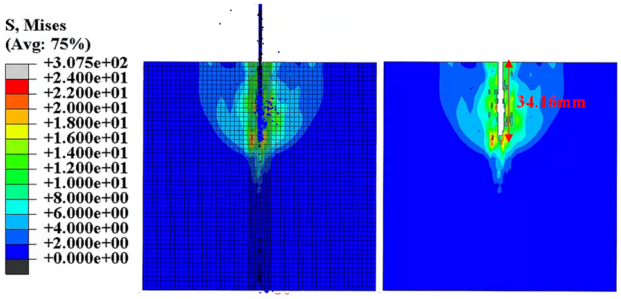

Figure 17. Simulation results with the horizontal movement speed of 300mm/min

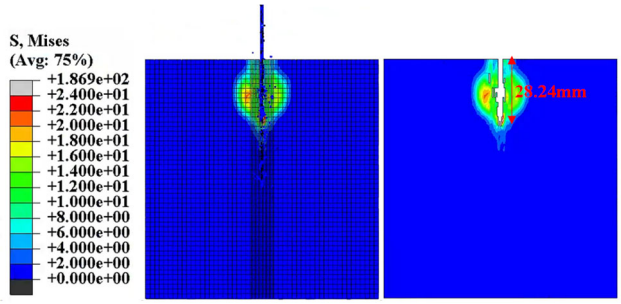

Figure 18. Simulation results with the horizontal movement speed of 400mm/min

The comparison of jet simulation cutting depth and single-factor test cutting depth at different horizontal movement speed is shown in Table 8.

Table 8. Results of model solution

V/(mm·min^{-1})	100	200	300	400	500	600
Actual cutting depth test (mm)	54.8	40.1	32.2	25.5	21.1	17.8
Simulated cutting depth (mm)	57.62	43.24	34.16	28.24	22.40	19.20

As shown in Figure 19, the jet simulation cutting depth generally decreases nonlinearly with increasing horizontal movement speed. As the waterjet horizontal movement speed increases, the cutting depth exhibits a boundary point change: when the horizontal movement speed is less than 200 mm·min-1, the rock cutting depth rapidly decreases; however, when the horizontal movement speed exceeds 200 mm·min-1, the rate of decrease in cutting depth slows down. With increasing horizontal movement speed, the number of abrasive particles impacting the rock per unit time decreases, reducing their impact capability and thus gradually decreasing the rock cutting depth. However, since the waterjet's destructive effect on the rock occurs within an extremely short time, the rate at which the cutting depth decreases becomes even slower as the horizontal movement speed continues to increase. When the horizontal movement speed is too low, it leads to waste of abrasive resources. Therefore, the inflection point where the rate of increase in rock cutting depth due to increasing waterjet horizontal movement speed is the optimal horizontal movement speed for the waterjet.

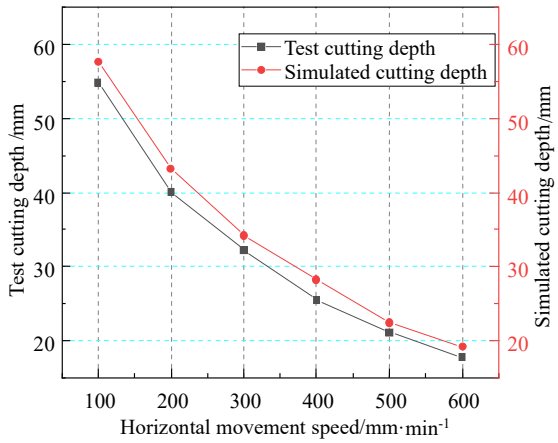

Figure 19. Comparison of experimental and simulated results of horizontal movement speed

4.6. Comparison And Analysis of Simulation Results and Experimental Results Under Different Abrasive Concentrations

Under conditions of jet pressure at 50 MPa, horizontal movement speed at 200 mm·min-1, cutting target distance at 10 mm, and impact angle at 90°, a Python script was used to randomly select grid nodes based on the proportion of abrasive particles, thereby altering the number of particles per unit volume to simulate changes in abrasive concentration during the experiment. The study analyzed how the depth of rock cuts varies with increasing abrasive concentration in waterjet cutting. Figures 20 and 21 illustrate the simulation results for abrasive concentrations of 8% and 12%, respectively.

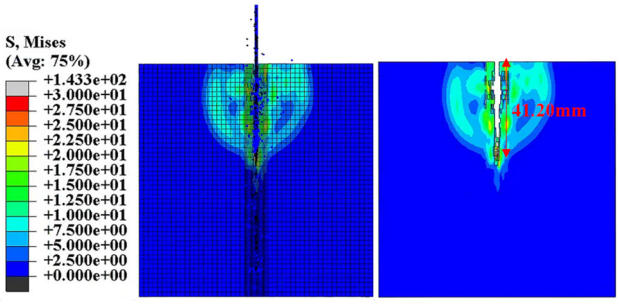

Figure 20. Simulation result graph for grinding abrasive concentration of 8%

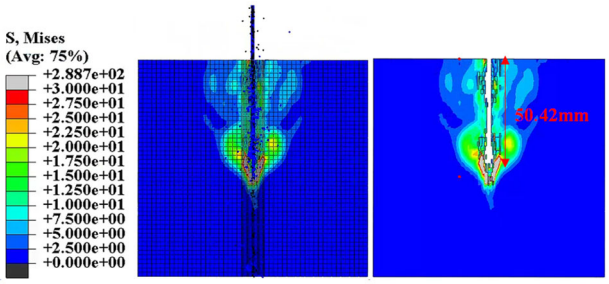

Figure 21. Simulation result graph for grinding abrasive concentration of 12%

The comparison of jet simulation cutting depth and single-factor test cutting depth at different abrasive concentrations is shown in Table 9.

Table 9. Results of model solution

C/%	4	8	12	16	20
Actual cutting depth test (mm)	32.8	36.4	46	41.5	37.3
Simulated cutting depth (mm)	35.12	41.26	50.42	52.12	53.42

As shown in Figure 22, the jet simulation cutting depth increases nonlinearly with the increase in abrasive concentration. When the waterjet abrasive concentration is between 4% and 12%, the number of abrasive particles is relatively low, leading to a lower collision probability, which is the main reason for the rapid increase in rock cutting depth with abrasive concentration. However, when the abrasive concentration exceeds 12%, the increase in rock cutting depth slows down as the abrasive concentration rises, due to the increased probability of abrasive particles colliding with each other, which somewhat reduces the impact kinetic energy of the waterjet. In practical applications, the waterjet abrasive concentration typically ranges from 5% to 20%, and higher abrasive concentrations can cause the nozzle to wear out more quickly. Therefore, the inflection point at which the rock cutting depth increases with waterjet abrasive concentration represents the optimal abrasive concentration for the waterjet.

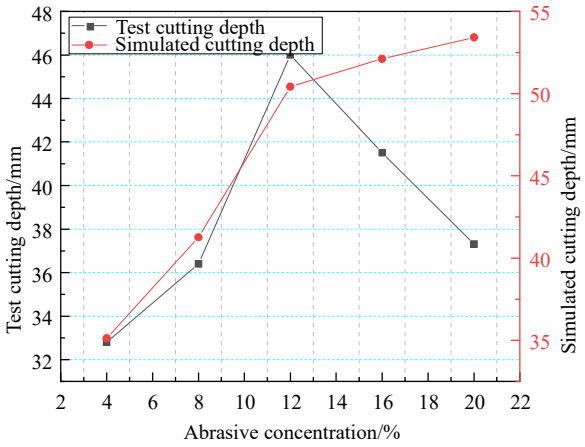

Figure 22. Comparison of experimental results and simulation results of abrasive concentration

4.7. Comparison And Analysis of Simulation Results and Experimental Results Under Different Cutting Angles

Under conditions of jet pressure at 50 MPa, horizontal movement speed at 200 mm·min^{-1}, cutting target distance at 10 mm, and abrasive concentration at 12%, different geometric models were established by varying the jet's inclination angle to analyze the changes in rock cutting groove depth with increasing waterjet cutting angle. Figures 23 and 24 show the simulation results for cutting angles of 80° and 90°, respectively.

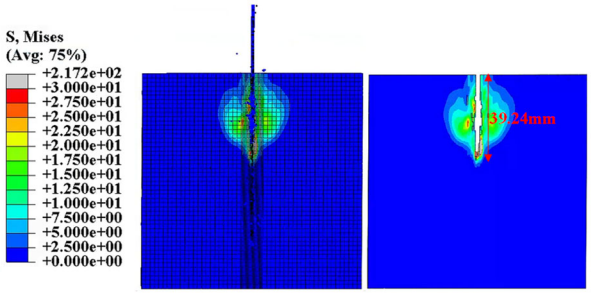

Figure 23. Simulation result graph for cutting angle of 80°

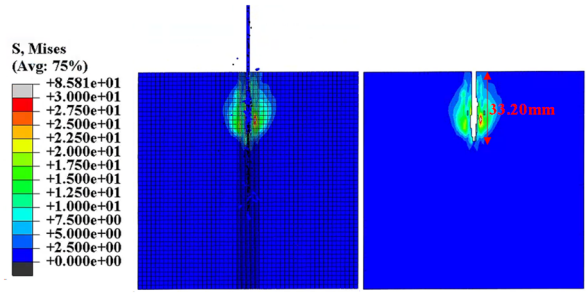

Figure 24. Simulation result graph for cutting angle of 90°

The comparison of jet simulation cutting depth and single-factor test cutting depth under different cutting angles is shown in Table 10.

Table 10. Results of model solution

δ/°	75	80	85	90	95	100	105
Actual cutting depth test (mm)	31.3	34.6	34.3	31.6	33.7	35.1	33.9
Simulated cutting depth (mm)	37.12	39.24	36.36	33.20	34.40	35.26	31.06

As shown in Figure 25, the cutting depth curve in the simulation is consistent with that of the experiment. At cutting angles of 80° and 100°, there are two peaks in the cut seam depth. The optimal cutting angle in the simulation matches the experimental result at 80°. Adjusting the cutting angle can reduce the rebound or deviation of abrasive particles from the jet path, thereby maintaining the concentration of the waterjet stream. The cutting angle significantly affects the rock-cutting effect of the waterjet, and choosing an appropriate cutting angle helps optimize the cutting process and improve the efficiency of the waterjet.

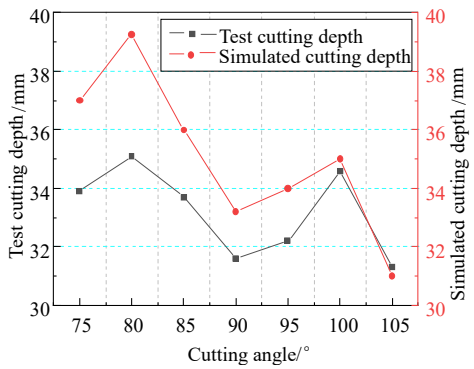

Figure 25. Comparison of cutting angle experiment and simulation results

5. Conclusions

(1) The results of the single-factor experiments on waterjet cutting of fine-grained sandstone indicate that there is a positive correlation between jet pressure and rock cut seam characteristic index, while there is a negative correlation with traverse speed. The cutting depth increases first and then decreases with the increase in cutting target distance and abrasive concentration. When cutting fine-grained sandstone, an optimal cutting target distance of 10 mm and an optimal abrasive concentration of 12% were found. As the cutting angle increases, two peaks in cutting depth occur at 80° and 100°, indicating that adjusting the cutting angle can significantly improve cutting efficiency.

(2) The results of the four-factor, five-level orthogonal experiment indicate that, with abrasive concentration fixed, the four key primary factors influencing cut depth are, in descending order: jet pressure > horizontal movement speed > cutting angle > cutting distance. The optimal process parameters for waterjet cutting of fine-grained sandstone are a jet pressure of 60 MPa, horizontal movement speed of 100 mm/min, cutting distance of 20 mm, and cutting angle of 85 degrees.

(3) Using regression analysis, a predictive model for the cutting depth of waterjet cutting fine-grained sandstone was

established. This model can enhance the cutting capability of waterjets in coal mine cutting operations and determine if the cut seam depth meets the cutting requirements. The SPH-FEM coupled method was used to simulate the effects of waterjet process parameters on the characteristics of the cut seams in fine-grained sandstone. Experimental validation revealed that numerical simulation could accurately replicate the cutting process by amplifying the traverse speed (with an error of 6.2%), uncovering the failure mechanism due to concentrated compressive stress in rock units within the jet impact area. The high correlation between numerical simulation and experimental results verified the model's reliability, providing references for setting experimental parameters and preliminarily exploring the influence of process parameters on the cutting depth of fine-grained sandstone. The research outcomes offer a safe and efficient non-explosive roof-cutting technology solution for coal mines' goaf retention, promoting the engineering application of green pressure relief processes, with significant economic and social benefits.

References

[1] GUO Juan, HU Rongbo, ZHOU Qizhong, et al. Outlook and overview of mineral resources situation of China in 2024 [J]. China Mining, 2025, 34(1): 37-45.

[2] LI MINGxuan, LIU Yong, WANG Yongjie, et al. Research on technology and application of hydraulic staged fracturing roof cutting and retaining roadway in hard roof [J]. China Mining, 2023, 32(12): 153-160.

[3] CHEN Ruijie, XIONG Zhiwen, WANG Rui, et al. Experimental study on the expansion law of hydraulic fracturing cracks in coal seam roof [J]. China Mining Science, 2024, 33(12): 208-216.

[4] LIU Xiaqing, WEI Shirong. Optimization of surrounding rock support parameters for shallow buried thick and hard roof coal seam roadway [J]. China Mining Science, 2024, 33(S1): 312-316.

[5] LIU Jianyu, ZHANG Lihui, BIAN Tao. Topping prevention and control technology of super-high fully mechanized face in extra thick coal seam [J]. China Mining Science, 2024, 33(z2): 265-269.

[6] CHEN Yong, ZHAO Rui, WU Zhen, et al. Study on deformation and failure law of surrounding rock of fully mechanized mining face passing through empty roadway group [J]. China Mining Science, 2025, 34(1): 154-163.

[7] LU Yiyu, HUANG Shan, GE Zhaolong, et al. Research progress and strategic thinking of coal mine water jet technology to enhance coal permeability in China [J]. Coal Engineering, 2022,47(9): 3189-3211.

[8] GONG Yongjun. Research status and Development trend of abrasive water jet cutting technology [J]. Chinese Hydraulics & Pneumatics, 2016(10): 1-5.

[9] DENG Songsheng, DAI Fei, PANG Cheng, et al. Discussion on safety application of abrasive water jet cutting technology in coal mine production [J]. Mining Safety and Environmental Protection, 2023,50(1): 115-118.

[10] Sun Lianxiang. Experimental Study on the Cutting Ability of High-Pressure Abrasive Water Jet for Hard Brittle Materials [D]. Harbin University of Technology, 2013.

[11] WANG Xiaochuan,LU Yiyu,KANG Yong,et.al. Experimental study of abrasive waterjet cutting coal-rock mass [J]. Journal of China University of Mining and Technology, 2011,40(2): 246-251.

[12] YU Yang. Experimental Study on Optimization of Abrasive Water Jet Cutting Process Parameters [D]. Dalian University of Technology, Mechanical Engineering, 2020.

[13] HU Yang. Research on Optimization of High-Pressure Water Jet Slotting Parameters for Unloading Deep Impact Coal Strata [D]. China University of Mining and Technology; China University of Mining and Technology (Jiangsu) Mining Engineering, 2022.

[14] GUO Jiahe, QI Xuyao, WANG Dong, et al. Influencing factors and depth prediction model of pre-mixed abrasive water jet cutting[J]. Chinese Journal of Safety Science, 2019,30(1): 101-106.

[15] HUA Yuchang. Theoretical and Experimental Study on the Cutting Depth of Pre-mixed Abrasive Water Jet Cutting for Grade 45 Steel [D]. Anhui University of Science and Technology, School of Mechanical Engineering, 2021.

[16] SONG Jinlai. Prediction and Experimental Study of Cutting Depth for Abrasive Water Jet Machining of Brittle Materials [D]. Harbin University of Technology, Mechanical Engineering, 2016.

[17] LIU Zhijiang. Study on rock breaking characteristics and influence of abrasive water jet based on SPH-FEM coupling algorithm [J]. Jilin Water Resources, 2024(2): 54-57.

[18] MING Jianyu, HUANG Fei, LI Shuqing, et al. Numerical Simulation Research on Post-mixing Abrasive Water Jet Impact Rock Breaking Based on SPH-FEM Coupling Algorithm [J]. Journal of Vibration and Shock, 2021, 40(16): 132-139.

[19] LI Jinghui. Experimental and Simulation Study on the Cutting Ability of Abrasive Water Jet for Marble [D]. Harbin University of Technology, Mechanical Engineering, 2015.

[20] MENG Xiangwang. Experimental and Simulation Study on Abrasive Water Jet Cutting of Brittle Materials [D]. Harbin University of Technology, 2014.

[21] Zhao Huihe. Research on the Performance of Abrasive Water Jet Rotary Slotting for Hard Rock [D]. China University of Mining and Technology, 2022.